VIROLOGY 189, 274–284 (1992)

Intracellular Processing of the N-Terminal ORF 1a Proteins of the Coronavirus MHV-A59 Requires Multiple Proteolytic Events

MARK R. DENISON,*,[1] PHILIP W. ZOLTICK,†,[2] SCOTT A. HUGHES,*,[3] BERNADETTE GIANGRECO,* ANN L. OLSON,‡ STANLEY PERLMAN,‡ JULIAN L. LEIBOWITZ,§ AND SUSAN R. WEISS†

*Departments of Pediatrics and Microbiology and Immunology, Jefferson Medical College of Thomas Jefferson University, Philadelphia, Pennsylvania 19107; †Department of Microbiology, University of Pennsylvania Medical School, Philadelphia, Pennsylvania 19104; ‡Departments of Pediatrics and Microbiology, University of Iowa, Iowa City, Iowa 52242; and §Department of Pathology and Laboratory Medicine, University of Texas Health Science Center, Houston, Texas 77030

Received January 2, 1992; accepted March 26, 1992

Several polypeptide products of MHV-A59 ORF 1a were characterized in MHV-A59 infected DBT cells, using antisera directed against fusion proteins encoded in the first 6.5 kb of ORF1a. These included the previously identified N-terminal ORF 1a product, p28, as well as 290-, 240-, and 50-kDa polypeptides. P28 was always detected as a discrete band without larger precursors, suggesting rapid cleavage of p28 immediately after its synthesis. Once p28 was cleaved there was little degradation of the protein over a 2-hr period. The intracellular cleavage of p28 was not inhibited by the protease inhibitor leupeptin, in contrast to results obtained during *in vitro* translation of genome RNA (Denison and Perlman, 1986). These data suggest that different protease activities may be responsible for the cleavage of p28 *in vitro* and *in vivo*. The 290-kDa protein was an intermediate cleavage product derived from a precursor of greater than 400 kDa. The 290-kDa product was subsequently cleaved into secondary products of 50 and 240 kDa. The intracellular cleavage of the 290-kDa polypeptide was inhibited by leupeptin at concentrations which did not inhibit the early cleavage of p28 or the cleavage of the 290-kDa product from its larger polyprotein precursor. In the presence of zinc chloride, a product of >320 kDa was detected, which appears to incorporate p28 at its amino terminus. This suggests that at least two protease activities may be necessary for processing of ORF1a proteins, one of which cleaves p28 and is sensitive to zinc chloride but resistant to leupeptin, and the other which cleaves the 290-kDa precursor and is sensitive to both inhibitors. Both the 290- and 240-kDa proteins should contain sequences predicted to encode two papain-like protease activities. © 1992 Academic Press, Inc.

INTRODUCTION

Mouse hepatitis virus (MHV), a murine coronavirus, contains the largest known viral RNA genome, a 31-kb, nonsegmented, single-stranded RNA of positive polarity (Pachuk *et al.*, 1989; Lee *et al.*, 1991). The replication strategy of MHV includes the transcription of a full-length negative-strand RNA from the input genome RNA, as well as the synthesis of subgenomic mRNAs. The subgenomic mRNAs form a 3′ coterminal (nested) set of seven RNAs (including genome length RNA) which extend varying distances in the 5′ direction. It is thought that only the 5′ most gene of each RNA is translated into protein. Gene 1 of MHV-JHM, a virus strain closely related to MHV A59, has been sequenced and found to be 21,798 nt in length (Lee *et al.*, 1991). It contains two open reading frames, ORF 1a and ORF 1b, which overlap by 75 nt, with ORF 1b in the -1 frame with respect to ORF 1a. A signal sequence present in this overlap region and a downstream pseudoknot formation can direct the ribosome to shift from the ORF1a to the ORF1b coding frame (Breedenbeek *et al.*, 1990; Lee *et al.*, 1991). Thus, gene 1 could potentially be translated into a polyprotein of >750 kDa.

Gene 1 most likely encodes the RNA-dependent RNA polymerase and other functions necessary for coronavirus RNA replication. MHV, like other positive-strand RNA viruses, does not contain a polymerase activity within the virion and must translate it from the input genome RNA. It is postulated, also by analogy to other positive-strand RNA viruses, that gene 1 is translated soon after infection into proteins containing various activities necessary for transcription and replication. Consistent with this model, *in vitro* translation of genome RNA results in only gene 1 products being detected (Leibowitz *et al.*, 1982; Denison and Perlman,

[1] To whom reprint requests should be addressed at Elizabeth B. Lamb Center for Pediatric Research, Department of Pediatrics, Vanderbilt University Medical Center, Nashville, TN 37232-2581.

[2] Current address: Department of Neurology, Thomas Jefferson University, Philadelphia, PA 19107.

[3] Current address: Department of Microbiology, University of Pennsylvania, Philadelphia PA 19104.

0042-6822/92 $5.00

1986). Further, gene 1 of the murine coronaviruses A59 and JHM, as well as of the avian coronavirus, IBV, has been shown to contain sequence motifs predicting polymerase, helicase and nucleotide triphosphate binding activities (Boursnell *et al.,* 1987; Gorbalenya *et al.,* 1989; Breedenbeek *et al.,* 1990; Lee *et al.,* 1991).

Genome RNA of MHV has been translated *in vitro* in a rabbit reticulocyte lysate, yielding a variety of polypeptides encoded in ORF 1a, including the N-terminal products p28 and p220, as well as p250, a precursor of p28 and p220. P250 is detected only in the presence of protease inhibitors (Leibowitz *et al.,* 1982; Denison and Perlman, 1986). Cleavage of p28, the extreme N-terminal ORF 1a product, is a delayed event *in vitro,* requiring a precursor of at least 160 kDa to be translated before cleavage occurs (Denison and Perlman, 1986; Soe *et al.,* 1987; Baker *et al.,* 1989). The cleavage of p28 *in vitro* may be autoproteolytic, effected by a protease activity encoded in the first 3.9–5.3 kb of ORF 1a (Baker *et al.,* 1989). More recent analyses indicates that this portion of MHV-JHM ORF 1a contains two distinct regions, predicted to encode papain-like proteases, and it has been suggested that one of these regions may be important in p28 cleavage (Baker *et al.,* 1989; Lee *et al.,* 1991).

Identification of gene 1 products and characterization of their processing and respective functions has been difficult to achieve in MHV-infected cells, probably due to a lack of effective antibodies. None of the protease, polymerase, helicase or metal binding activities predicted by analysis of the gene 1 sequence have been detected *in vivo* (Gorbalenya *et al.,* 1989; Lee *et al.,* 1991; Denison *et al.,* 1991). To this point the only gene 1 product identified in MHV-A59-infected cells has been p28, which was detected at late times after infection by two-dimensional protein gel electrophoresis (Denison and Perlman, 1987). The kinetics and cleavage reaction of p28 *in vivo* were not investigated in that report.

It is important to define the pattern of translation and processing of ORF 1a, as well as the specificity of any cleavage events which may occur in order to better understand the number and type of proteases which may be active in coronavirus replication, as well as to putative polymerase gene products. In this report we describe the intracellular synthesis and processing of p28 and other ORF 1a polypeptides in MHV-infected cells. We have characterized the kinetics of synthesis of these products, their precursor–product relationships and the sensitivities of the cleavage reactions to protease inhibitors. Our results suggest that the intracellular ORF 1a products may be substantially different from those identified from *in vitro* translation of genome RNA, and that more than one protease activity may be necessary for the processing of ORF 1a translation products.

MATERIALS AND METHODS

Infection of DBT cells with MHV A59

Confluent monolayers of DBT cells were infected with MHV-A59 in 60-mm petri dishes at an m.o.i. of 10 PFU/cell in DMEM 2% FCS for 30 min at 37°. Excess virus and media were removed and the cells were incubated in DMEM without methionine (GIBCO) with 2% FCS for the remainder of the experiment. Actinomycin D (Sigma) was added to the media at 2 hr postinfection (pi) to a final concentration of 10 μg/ml. Polypeptides were labeled with [^{35}S]methionine (Translabel-ICN) at a concentration of 200 μCi/ml for periods as indicated in individual experiments. Label was added at 7.5 hr pi unless otherwise indicated. The duration of incubation with label varied by experiment, but generally 1.5 to 2 hr gave maximum incorporation of label into in viral polypeptides.

Synchronization of translation in virus-infected cells

Initiation of translation was blocked by increasing the NaCl concentration in the overlying medium by 200 m*M* above that contained in DMEM (GIBCO), as described by Saborio *et al.* (1974). Under usual conditions, the cells were incubated in the hypertonic NaCl for 30 min, before replacing the high salt medium with isotonic medium containing [^{35}S]met.

Preparation of whole cell lysates of A59-infected cells

At the times indicated in individual experiments, the media was removed and the cells were placed on ice, washed twice with 150 m*M* Tris–HCl, pH 7.4, and swollen in 10 m*M* Tris–HCl, pH 7.4, for 30 sec on ice. Following removal of the 10 m*M* Tris, the cells were lysed by the addition of 300 μl/plate (2.5×10^6 cells) of a solution containing 1% NP40, 1% sodium deoxycholate, 1% SDS, 150 m*M* NaCl, and 10 m*M* Tris, pH 7.4 (Buffer A). Phenylmethylsulfonylfluoride (PMSF) ately prior to use. After incubation on ice for 3 min and observation for complete lysis, lysates were frozen at −70° until use.

Preparation of antibodies for immunoprecipitation

The polyclonal anti-peptide serum (αp28p) was raised in a rabbit against a 14 amino acid synthetic oligopeptide (amino acids 25 to 38 from the initiating

methionine of JHM ORF 1a), which is within the region coding for p28 (Table 1). In addition, polyclonal antisera directed against polypeptides encoded in the first 6.5 kb of ORF 1a (antisera 81043 and 600A) were also utilized. These antisera were raised in rabbits using as an immunogens procaryotic/viral fusion proteins (Zoltick *et al.*, 1989; Denison *et al.*, 1991). The locations of the cDNAs encoding the fusion proteins used to raise these antisera are shown in Table 1. The hybridoma cell line secreting antibodies against the S protein (JA3.10) was obtained from Dr. John Fleming at the University of Wisconsin. The hybridoma cell line, 1.16.1, secreting antibodies against N (nucleocapsid) was used as previously described (Denison *et al.*, 1991). Antibodies were prepared for immunoprecipitation reactions by binding them to Protein A (PrA)–Sepharose beads (Sigma) in 1 ml of an immunoprecipitation buffer, identical to the lysis buffer but containing only 0.1% SDS (buffer B). For individual immunoprecipitation reactions, 5 μl of the polyclonal antisera or 50 μl of the monoclonal antisera were incubated with 30 μl of swollen PrA–Sepharose beads for 2 hr with rocking at 4°, followed by 3 washes in buffer B.

Immunoprecipitation of ORF 1a translation products from whole cell lysates

Whole cell lysates, prepared as described above, were thawed on ice and DNA was sheared by 10 passages through a 23-gauge needle. Debris was pelleted by centrifugation at 13,000 rpm for 10 min at 4°, and the supernatant was transferred to a fresh microfuge tube. Typically, 150 to 300 μl (1.25 to 2.5 $\times$ 10^6 cells) was used for each immunoprecipitation reaction. Lysates were diluted to 1 ml in immunoprecipitation buffer, identical to the lysis buffer, but lacking SDS (buffer C), resulting in final SDS concentrations of 0.1%. Lysates were precleared with preimmune serum-armed beads (30 μl per reaction) for 2 hr at 4°, the beads were pelleted, and the supernatant was transferred to a fresh microfuge tube and incubated with PrA–Sepharose beads armed with specific antisera. Following the incubations, the supernatant was discarded and the beads were washed 4 times with alternating high and low salt rinses (buffer B containing either 150 m*M* or 1 *M* NaCl). After rinsing, 50 μl of 2× Laemmli buffer (Laemmli, 1970) was added to the pelleted beads, which was boiled for 5 min at 100° prior to electrophoresis of the supernatant, usually on 5–18% gradient SDS–polyacrylamide gels (gSDS–PAGE).

In vitro translation of A59 genome RNA in a rabbit reticulocyte lysate

Purification of A59 genome RNA, translation in rabbit reticulocyte lysate, immunoprecipitation, and electrophoresis were all performed as previously described (Denison *et al.*, 1991).

TABLE 1

ANTISERA USED FOR IMMUNOPRECIPITATION OF A59 ORF 1A PRODUCTS

Antiserum	Peptide type	Peptide size (aa)	cDNA for fusion spans nucleotides
αp28p	Oligopeptide	14	N/A
81043	Fusion protein	~400	2879–3968[a]
600A	Fusion protein	~466	5000–6486[a]

[a] Antisera were directed against fusion proteins encoded by cDNAs from these regions of gene 1 of MHV-A59. The exact 5′ end of 600A cDNA has not been determined.

Molecular mass estimates of ORF 1a polypeptides

Estimates of molecular mass were derived by a modification of the method described by Lamblin (Lamblin and Fine, 1979; Lamblin, 1978; Lamblin *et al.*, 1976). Immunoprecipitation products were analyzed on 4–10% polyacrylamide gels in the presence of increased bisacrylamide (30% T/3.8% C) using as standards nonreduced α2 macroglobulin, thyroglobulin, fibrinogen, and IgM, as well as high molecular weight standards (SDS-6H, Sigma). A regression curve of log MW vs log %T was derived from standards and used to estimate the molecular weight and error of ORF 1a products.

RESULTS

Immunoprecipitation of MHV-A59-infected cells with ORF 1a antisera

A59-infected cells were labeled for 2 hr at late times of infection (6–8 hr). Whole-cell lysates were immunoprecipitated with antisera αp28p, 81043, or 600A (see Materials and Methods) and also with monoclonal antibodies to structural proteins N (αN) and S (αS) (Fig. 1). The nucleocapsid and spike proteins were easily detected at this time pi, consistent with the presence of virus-induced syncytia formation in the cell monolayer and increasing titers of MHV-A59 in the supernatant media. The polyclonal antiserum directed against a synthetic oligopeptide within the sequence coding for p28 (αp28p) (Table 1) precipitated a 28-kDa polypeptide, which migrated with the same mobility as p28 synthesized during *in vitro* translation of A59 genome RNA. The 28-kDa band which was detected in infected DBT cells was not precipitated by preimmune serum, αN, or αS, nor was any band of similar mobility detected by αp28p in uninfected DBT cells. Despite the

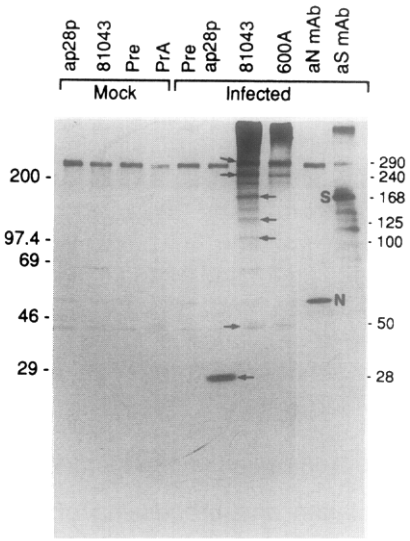

FIG. 1. Immunoprecipitation of A59 ORF 1a products. Immunoprecipitates of [^{35}S]met-labeled, A59-infected cells were analyzed by 5–18% gradient polyacrylamide gel electrophoresis (gSDS–PAGE). Mock indicates mock-infected cells. Antisera are as described in Table 1 (αp28p, 81043, and 600A). Controls include preimmune sera (Pre), Protein A–Sepharose beads without antibody (PrA), and anti-N (αN mAb) and anti-S (αSmAb) monoclonal antibodies. Molecular mass markers are to the left of the gel and sizes of specific precipitation products are to the right of the gel, with arrows indicating these products.

long labeling period (2 hr) and the intensity of the label (200 μCi/ml of [^{35}S]met), only p28 was detected. No potential precursors to p28 were detected, with all larger bands being nonspecific products also precipitated by preimmune serum from infected and uninfected DBT cells. Neither antiserum 81043 nor 600A detected p28. This was expected since they were directed against sequences encoded downstream of p28 (Table 1, see also Fig. 6), and indicated that none of the downstream ORF 1a products was a p28 containing precursor. This was in contrast to the results from *in vitro* translation of A59 genome RNA, in which p28-containing precursors from 160 to 250 kDa were easily detected by αp28p (Denison *et al.*, 1991). These results suggested that p28 was more rapidly cleaved *in vivo* than *in vitro.*

Antisera 81043 and 600A both detected major products with molecular masses of approximately 290 kDa (p290) and 240 kDa (p240), as well as a large, heterogeneous accumulation of radioactivity with electrophoretic mobility of greater than 400 kDa (Fig. 1). The sizes of these proteins were determined as described under Materials and Methods, with a mean error of 10%. Antiserum 81043 detected a variety of smaller bands of approximately 168, 125, and 100 kDa. Neither αp28p nor 600A detected these polypeptides. Finally, antiserum 81043 precipitated a polypeptide at 50 kDa (p50), which was not precipitated by αp28p. This product was variable in amount and migrated immediately above a nonspecific band between 46 and 50 kDa which was precipitated by all antisera utilized, including 81043 and 600A. P50 could only be detected as a discrete band by 81043 as is most clearly delineated in Figs. 3 and 5A. The detection of p50 by 81043 but not 600A suggested that p50 was either located 5′ to p240 or was a N-terminal cleavage product of a larger polyprotein spanned in part by 81043.

Time of appearance of ORF 1a products

DBT cells were infected at a high m.o.i. (50 PFU cell) at 4° for 1 hr to ensure complete, synchronous, and single cycle infection and were labeled with [^{35}S]Met in the presence of actinomycin D for serial 1.5-hr periods from 0 to 9 hr. Syncytia were first observed on the infected cell monolayer at 6 hr pi and progressed to 90–100% confluency by 8 hr pi. The first products specific to ORF 1a were contained in a diffuse region of increased incorporation at the top of the gel, immunoprecipitated by antiserum 81043 (Fig. 2B). This heterogeneous band was also detected using antiserum 600A, but was not precipitated by αN, or αp28p (Figs. 2A and 2C), nor by αS (data not shown), supporting the conclusion that this was not nonspecific aggregation of structural proteins. By 3–4.5 hr pi, this heterogeneous band of >400 kDa had increased significantly, and p28, p290, and p240 were readily detected. One additional polypeptide of approximately 170 kDa was precipitated by αp28p (Fig. 2A, 4.5–6 hr). This band was also precipitated by preimmune rabbit serum in infected cells, at the same time point and from the same lysate (Fig. 2D), indicating that it was a nonspecifically precipitated product, possibly S, rather than a p28 containing precursor. Additionally, it was not seen at subsequent time points, nor in any other experiments using αp28p antisera. Nucleocapsid was also observed by 3–4.5 hr pi, well before the presence of virus-induced syncytia formation. All of the MHV-specific products increased in amount during subsequent labeling periods, until 7.5–9 hr pi, when the amount of precipitated products was diminished. At this latter labeling period there was decreased cell viability and loss of syncytia from the cell monolayer.

Precursor–product relationships of ORF 1a products

In order to more completely define the precursor–product relationships among the ORF 1a products, pulse chase labeling of infected DBT cells was performed at late times of infection, when synthesis of ORF 1a products was maximal (50–60% of monolayer

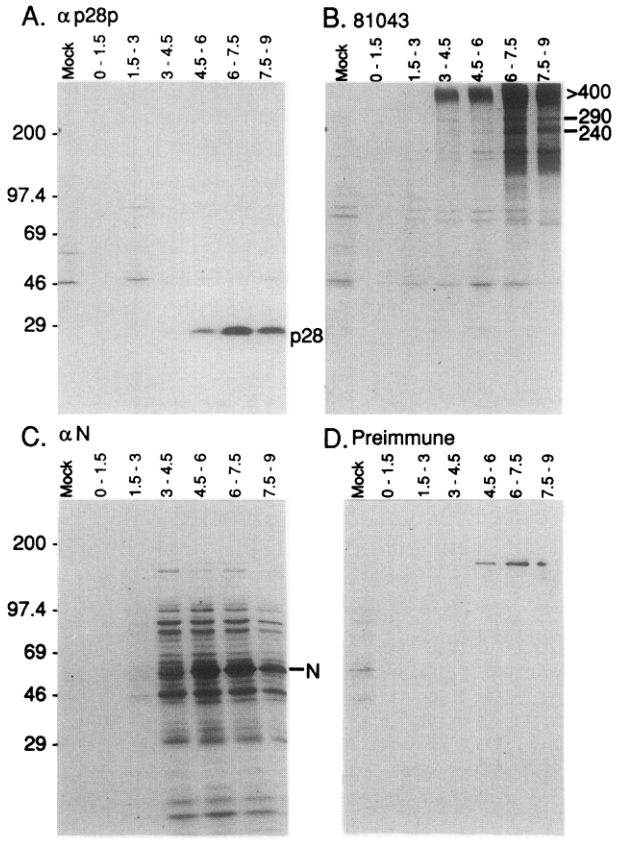

FIG. 2. Pulse labeling of ORF 1a polypeptides at different times postinfection. [^{35}S]met was added to the media for 1.5-hr periods at the times pi indicated above the lanes. Lysates of infected cells were immunoprecipitated with antisera (A) αp28p, (B) 81043, (C) αN, and (D) preimmune rabbit serum, and analyzed by 5–18% gSDS–PAGE. "Mock" indicates mock-infected cells labeled from 0–4 hr pi. Molecular mass markers are to the left of the gels. The estimated masses of specific immunoprecipitation products are shown on the gel.

involved in syncytia formation). A59-infected cells were labeled with [^{35}S]met for 20 min and then chased with excess cold methionine for 0–120 min, lysed, and immunoprecipitated with antisera αp28p, 81043, or 600A (Fig. 3). As in Figs. 1 and 2, αp28p precipitated only p28 with no detectable precursors. The amount of p28 detected remained constant up to 120 min of chase, with no evidence of processing or degradation. All three antisera detected a band migrating at 278 kDa, just below the 290-kDa virus-specific ORF 1a product (Fig. 3, 15 min, 600A). This was a nonspecifically precipitated cellular polypeptide, detected in infected and mock-infected cells by all antisera including preimmune serum (see also Fig. 1). At the end of the 15-min labeling period (0 min lane), a majority of the labeled products precipitated by both 81043 and 600A were in the heterogeneous band of greater than 400 kDa. The 290-kDa band was first detected by both antisera at 15 min of chase. Subsequently, the 240- and 50-kDa products were first detected at 30 min of chase. Antiserum 600A detected the 290- and 240-kDa products, but not the 50-kDa product, consistent with the results in Figs. 1 and 2. The sizes of these products, as well as the late, simultaneous appearance of the 240- and 50-kDa products, suggested that they were derived from the 290-kDa polypeptide by a delayed cleavage reaction (50–90 min), with p50 as the amino terminal product and p240 as the carboxy terminal. The 168-, 125-, and 100-kDa polypeptides detected by 81043 appeared simultaneously at 0–15 min, suggesting that they were products of premature translation, which were not processed.

Synchronized translation of p28 in infected DBT cells

Since translation and processing of viral polypeptides were not synchronous at late times pi, intracellular translation of MHV RNA was synchronized with hypertonic NaCl, in order to confirm the kinetic relationship between the 28-, 290-, 240-, and 50-kDa ORF1a products, (Fig. 4). The presence of excess (200–220 m*M*) NaCl has been shown to almost entirely block reinitiation of translation on mRNAs, without affecting polypeptide chain elongation or termination (Saborio *et al.*, 1974). In both uninfected and A59-infected DBT cells, 200 m*M* excess NaCl was necessary to completely block incorporation of [^{35}S]Met into cellular or viral polypeptides (Fig. 4A). This block appeared to be complete within 10 min of addition of excess NaCl. When [^{35}S]Met was added at the time when the hypertonic block was removed and isotonic conditions re-

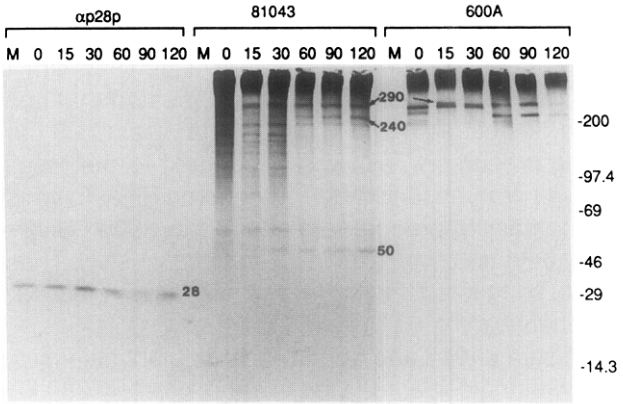

FIG. 3. Pulse chase labeling of ORF 1a products. At 7 hr pi, viral polypeptides were labeled for 15 min with [^{35}S]Met, followed by a chase with excess unlabeled methionine for the times in minutes indicated above the lanes. Time 0 min indicates the end of the labeling period. Cell lysates were immunoprecipitated with antisera as indicated above groups of lanes. Mock-infected cells (M) were labeled for 15 min and chased for 60 min before lysis and immunoprecipitation. Molecular mass markers are to the right of the gel. Specific immunoprecipitation products are indicated on the gel.

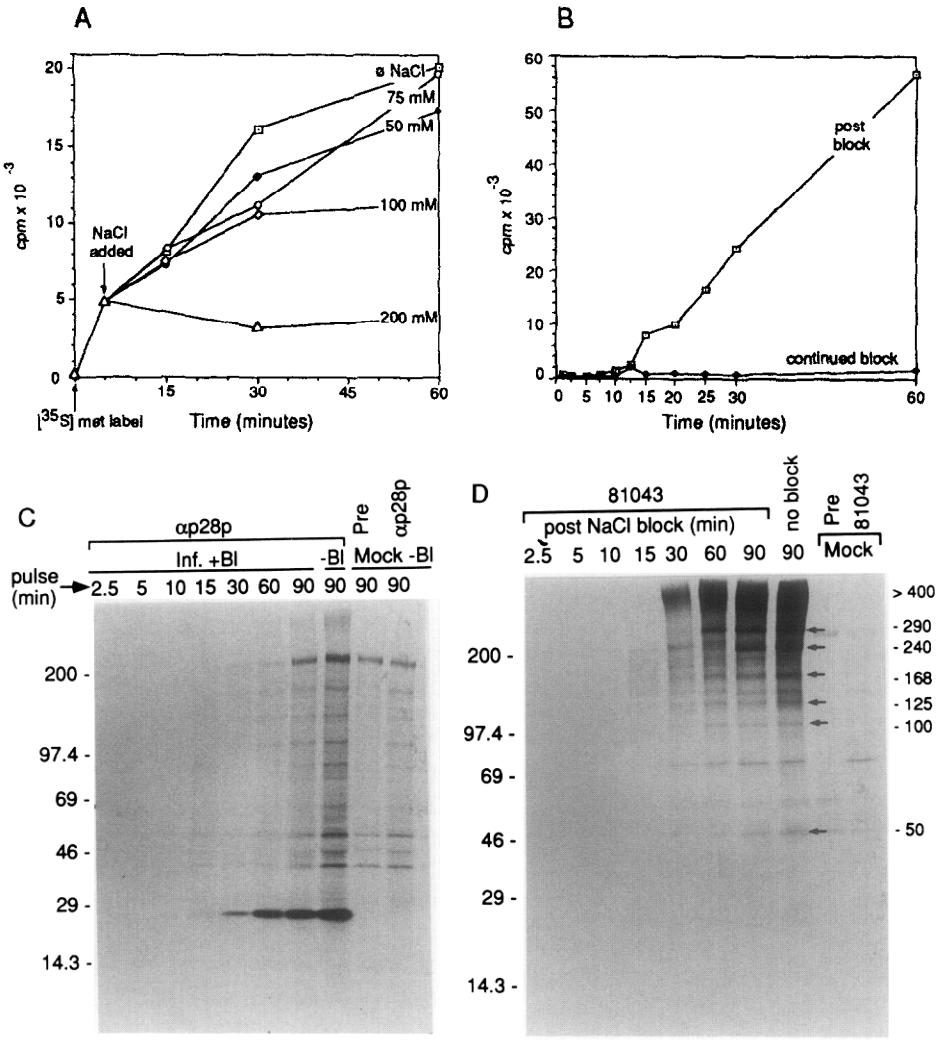

FIG. 4. Synchronized pulse-labeling of ORF 1a products following hypertonic block. (A) [^{35}S]met incorporation into TCA precipitable products in MHV A59-infected DBT cells following addition of hypertonic NaCl. [^{35}S]Met was added at Time 0 min and incubated with cells for 60 min. Excess NaCl was added 5 min after addition of label and maintained for the remainder of the experiment. Final concentrations of NaCl are shown along the curves of TCA incorporation. (B) Uptake of [^{35}S]Met into TCA precipitable products after removal of hypertonic block. [^{35}S]met was added to cells in an isotonic media following the removal of media containing 200 m*M* excess NaCl (Time 0 min), and samples were taken for TCA-precipitable counts at the times indicated, either in the absence or the presence of continued hypertonic NaCl. (C and D) At 7 hr pi, infected cells were subjected to 200 m*M* excess NaCl for 30 min, followed by restoration of isotonic conditions and the addition of [^{35}S]met to the media for the times in minutes indicated above the lanes (2.5–90). Infected cells lysates were immunoprecipitated with antiserum αp28p (C) or 81043 (D). As a control, infected cells were labeled for 90 min without hypertonic block (no block, −Bl) and immunoprecipitated with either αp28p or 81043. In addition, mock-infected cells (mock) were subjected to hypertonic block as above and labeled for 90 min prior to lysis and immunoprecipitation with αp28p, 81043, or preimmune rabbit serum (Pre). Molecular mass markers are to the left of the gels. Specific bands are indicated by arrows.

stored, there was a delay of 7.5–15 min before significant incorporation into TCA precipitable products occurred (Fig. 4B). The cells where the hypertonic block was maintained after addition of label showed no uptake during the entire labeling period. Based on these initial experiments, 200 m*M* NaCl was added to the overlying media for 30 min, after which the hypertonic media was removed and the cells were labeled in isotonic media for increasing periods of time, prior to lysis, and immunoprecipitation with αp28p, 81043, or preimmune serum. P28 was the only MHV product detected by αp28p (Fig. 4C). It was detected by 15 min after restoration of isotonic conditions, well before the much larger, 81043 precipitated heterogeneous band of >400 kDa, which was first seen after 30 minutes of labeling (Fig. 4D). Although our preliminary experiments demonstrated a lag period before incorporation of label recommenced, it was clear that no p28 con-

taining precursors were present even in conditions of synchronous translation, supporting the conclusion that p28 was cleaved prior to the synthesis of the downstream ORF 1a products. This was in marked contrast to our results from immunoprecipitation of pulse-labeled *in vitro* translation products of genome RNA, in which polypeptides of 60–220 kDa accumulated for up to 45 min before the first appearance of p28 (Denison and Perlman, 1986; Denison *et al.*, 1991).

Following accumulation of label into the heterogeneous band of greater than 400 kDa at 30 min of label, the 290-kDa band appeared abruptly at 60 min, followed by the simultaneous appearance of the 240- and 50-kDa products by 90 min (Fig. 4D). These data suggested that the 290-kDa product was also a late cleavage product of a larger precursor. p290 then required up to an additional 30 min for secondary cleavage into products of 240 and 50 kDa. The other virus specific polypeptides at 168, 125, and 100 kDa again gradually accumulated during the pulse-labeling period, but demonstrated no detectable precursor–product relationships, in agreement with the results of the nonsynchronized translation.

Effect of protease inhibitors on the cleavage of ORF 1a precursors

The proteolytic cleavage patterns of ORF 1a products were assessed by adding the protease inhibitor leupeptin to the infected cells at late times pi, but prior to the addition of [^{35}S]Met label (Fig. 5A). Leupeptin, a low molecular weight (455 Da) reversible inhibitor of trypsin-like serine proteases, as well as some cysteine proteases, effectively blocks the proteolytic cleavage of p28 during *in vitro* translation of A59 genome RNA at concentrations of 1–2 m*M* (Denison and Perlman, 1986). Leupeptin has been shown to penetrate intact cells (Appleyard and Tisdale, 1985). MHV A59-infected DBT cells were labeled in media containing 2 m*M* leupeptin followed by immunoprecipitation with preimmune serum, αp28p, 81043, or 600A. The cleavage of p28 *in vivo* was not inhibited by the presence of up to 2 m*M* leupeptin in the media. These results differed substantially from those obtained in the cell-free rabbit reticulocyte lysate, in which the cleavage of p28 from its precursors was almost completely inhibited by 2 m*M* leupeptin (Denison and Perlman, 1986; Denison *et al.*, 1991), resulting in increased detection of p28-containing precursors, specifically p250. In contrast, the 240- and 50-kDa bands precipitated by 81043 in the absence of leupeptin were not detected when ORF 1a products were labeled in the presence of leupeptin. An identical pattern was observed in the products precipitated by 600A, with the exception that the 50-kDa product was not detected by this antibody under any circumstances. In addition, the 290-kDa band was significantly more dense in the presence of leupeptin as detected by both antibodies, as would be expected if its cleavage into products of 240 and 50 kDa were prevented. Finally, the 168-, 125-, and 100-kDa products were not altered in electrophoretic mobility nor relative amount detected by the addition of leupeptin to the cells, supporting the conclusion that these were minor products derived from premature termination of translation rather than post-translational cleavage.

Since the cleavages of p28 and the 290-kDa product were not detectably inhibited by leupeptin, the experiment was repeated, instead using E64 (Sigma), a specific, irreversible cysteine protease inhibitor, and also using $ZnCl_2$, which completely inhibits p28 cleavage *in vitro* at 1 m*M* concentrations (Denison and Perlman, 1986; Denison and Perlman, 1987). E64 had no detectable effect on the proteolytic processing of any of the identified ORF 1a products (data not shown), even though it is a small MW inhibitor and has been shown to be able to penetrate cells (Gordon and Seglen, 1989). It is not clear whether this lack of inhibition was the result of insensitivity of the protease activities to E64 or was due to insufficient intracellular concentrations. Zinc chloride had a very low working concentration range in the media, with 0.05 m*M* producing no inhibition of cleavages of the ORF 1a products and 0.2 m*M* causing visible toxicity to the cell monolayer and almost complete inhibition of translation of MHV polypeptides. At a $ZnCl_2$ media concentration of 0.1 m*M*, there was a decrease in detectable p28, as well as the appearance of a new band of >320 kDa (Fig. 5B). A polypeptide of identical mobility was also detected by antisera 81043 and 600A in the presence of 0.1 m*M* $ZnCl_2$, the only band which was detected by all three antisera, suggesting that $ZnCl_2$ to a limited extent inhibited the cleavage of p28 from the growing polyprotein precursor, resulting in a product which contained epitopes recognized by each of the three antisera.

DISCUSSION

This report represents the first description of the processing of p28 in MHV-infected cells, as well as the first description of intracellular ORF 1a products encoded downstream of p28. ORF 1a products were easily detectable by 3 hr pi and continued to be synthesized throughout the infectious cycle in increasing amounts until late in infection, when there was a diminution of the amounts detected. Gene 1, ORF 1a products should be the first proteins synthesized after uncoating of the virion RNA in the cytoplasm, and the failure to detect them prior to 1.5 hr pi was probably due to the low copy number of input genome RNA avail-

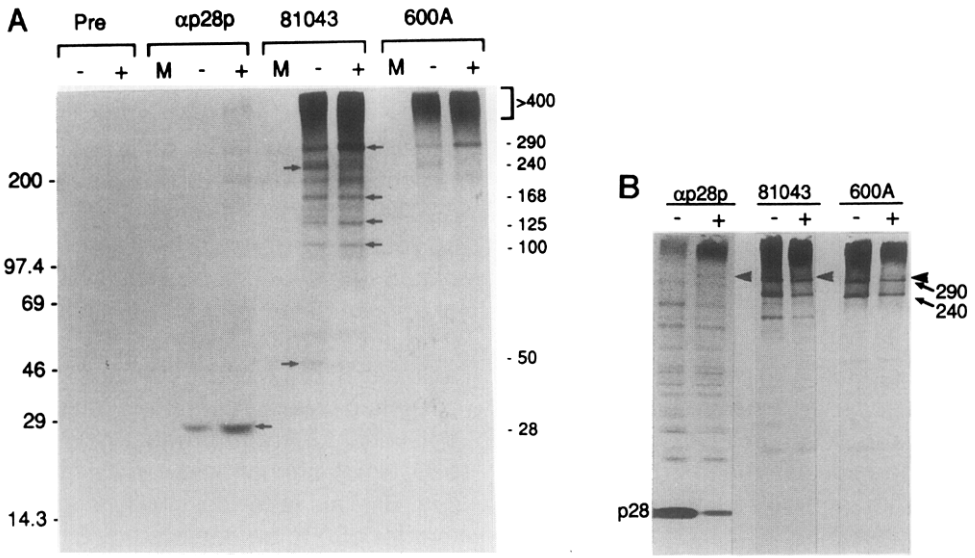

FIG. 5. Inhibition of proteolytic cleavage of ORF 1a precursors. (A) At 7 hr pi, leupeptin (2 m*M*) was added to the supernatant media for 30 min prior to the addition of [^{35}S]Met for an additional 90 min. Cell lysates were immunoprecipitated with antisera as indicated above the lanes. Infected cells were labeled in the presence (+) or the absence (−) of leupeptin. Mock-infected cells (M) were labeled in the absence of leupeptin. Preimmune serum (Pre) was used as a control. Predicted molecular masses of specific ORF 1a products are to the right of the gel, with arrows indicating the respective bands. Molecular mass markers are to the left of the gel. (B) Infected cells were labeled with [^{35}S]met in the absence (−) or presence (+) 0.1 m*M* zinc chloride. Lysates were precipitated with antisera αp28p, 81043, or 600A as indicated above groups of lanes. Specific ORF 1a products are indicated. Bold arrowheads indicate product of 320–350 kDa seen in the presence of zinc chloride.

able for translation. These data suggest a model in which small amount of ORF 1a gene products are translated from input genome RNA until 1.5–3 hr pi, when copies of genome RNA begin to be transcribed and become available as templates for translation of ORF 1a products, allowing much greater quantities to be produced. This model is supported by the fact that nucleocapsid protein, the product of subgenomic mRNA 7, demonstrated similar kinetics of appearance. A model of translation of ORF 1a products from progeny genome RNA is also supported by studies which have demonstrated that continuous *de novo* protein synthesis is necessary for efficient RNA synthesis during virus replication (Sawicki and Sawicki, 1986; Perlman *et al.*, 1987). It is also possible that the increased detection late in infection of all ORF 1a products may have been partially the result of intracellular accumulation, since it was demonstrated that all of the polypeptides were stable for at least 2 hr. The terminal diminution in amounts detected probably resulted from loss of cell numbers and viability late in infection, since at that time 100% of cells were involved in syncytia and were beginning to be lost from the plate.

Synthesis and processing of p28

Data from *in vitro* translation of MHV-JHM ORF 1a transcripts indicate that p28 is cleaved *in vitro* by a *cis*-autoproteolytic mechanism (Baker *et al.*, 1989). We were unable to analyze the initial cleavage events in infected cells, since at earliest times pi the quantity of ORF 1a products present was below the level of detection by the available antisera. It is therefore quite possible that the cleavage of p28 in A59-infected cells at very early times pi may occur by an autoproteolytic mechanism similar to that described during *in vitro* translation. However, the data presented here indicate that intracellular processing of p28 at late times pi may be effected by an additional or alternative mechanism. We detected no p28-containing products of 140 to 180 kDa, *in vivo*, which would be necessary to span the predicted papain-like protease regions (Lee *et al.*, 1991). The antiserum αp28p detected only p28 under all conditions of labeling and immunoprecipitation utilized, supporting the conclusion that early, rapid cleavage of p28 was the predominant method of genesis late in infection. In contrast, the processing of p28 from larger N-terminal precursors is easily detected in the rabbit reticulocyte cell-free translation system, in which p28 is clearly not cleaved *in vitro* until at least 160 kDa of protein has been synthesized (Denison and Perlman, 1986; Soe *et al.*, 1987; Baker *et al.*, 1989). We were able to detect *in vitro* all p28-containing precursors up to 250 kDa utilizing αp28p and thus do not believe that epitope masking could account for the lack of p28 containing-precursors *in vivo* in our experiments.

Another difference between the processing of p28 *in vitro* and *in vivo* was the sensitivity of its cleavage reaction to inhibition by protease inhibitors. During the *in vitro* translation of A59 genome RNA, the cleavage of p28 is sensitive to inhibition by leupeptin, with essentially complete inhibition of proteolysis occurring at 2-mM concentrations. In contrast, the cleavage of p28 in infected cells was unaffected by leupeptin, even though leupeptin was clearly able to penetrate cells and inhibit the cleavage of other ORF 1a precursor polypeptides. Both of the predicted papain protease activities, as well as a predicted 3C-like protease in ORF 1a of JHM, are postulated to be cysteine proteases, which should be inhibited by leupeptin or E64. There is not yet enough data to determine whether this rapid cleavage of p28 resulted from intramolecular self-cleavage of p28, such as that described in several of the nonstructural proteins of the picornaviruses (Krausslich and Wimmer, 1988; Palmenburg, 1990), from one of the described ORF 1a *cis*-protease activities (Baker *et al.,* 1989) which may be acting *in trans* within the infected cell, or from an as yet unrecognized viral or cellular transacting protease.

Synthesis and processing of ORF 1a products downstream from p28

The products of ORF 1a in A59-infected DBT cells appear to be derived from a large polyprotein precursor through at least three independent proteolytic events (Fig. 6). The first event was the cleavage of p28 from the growing polypeptide chain. Translation on the genome RNA template continued with the synthesis of a variety of products greater than 400 kDa in size. It is not clear whether these large precursors terminated at the end of ORF 1a or were composed of ORF 1a–1b fusion polypeptides. It is possible that both were present, based on the demonstrated efficiency of ribosomal frameshifting in the coronaviruses (Brierley *et al.,* 1987; Breedenbeek *et al.,* 1990; Lee *et al.,* 1991). The probability that ORF1a–1b fusion protein precursors are synthesized is also supported by the fact that up to 60 min of labeling was required for discrete ORF1a products other than p28 to be detected, which was ample time for translation of almost the entirety of ORF1a and ORF1b. The polyprotein was cleaved at 45–60 min into a primary product of 290 kDa. This primary cleavage product was subsequently proteolyzed into secondary products of 50 and 240 kDa.

Such hierarchical proteolytic patterns have been well described both for the alphaviruses (de Groot *et al.,* 1990) and the picornaviruses. Analysis of the JHM ORF 1a sequence does not predict any regions with similarity to the conserved alphavirus cleavage sites [G, (A, C, G), (A, G, Y)] which could account for the ORF 1a products identified. However, there are several regions of the ORF 1a sequence with similarity to known picornavirus 3C protease substrate sites. One of these sites, the lys-arg (KR) at aa 3160–3161, was previously described as a potential cleavage site for the putative 3C-like protease activity in ORF 1a (Lee *et al.,* 1991). A polypeptide extending from the predicted C terminus of p28 to the KR dipeptide at 3160 would have a mass of approximately 323 kDa. This is substantially larger than the 290-kDa polypeptide actually precipitated by antisera 81,043 and 600A and suggests that either p290 is cleaved at a more 5′ cleavage site or that an additional cleavage product exists between p28 and p50, which cannot be detected by the antisera utilized (Fig. 6). This latter possibility is supported by the fact that for p50 to be detected by 81043, its carboxy terminus would have to extend beyond aa889, thus leaving a gap of approximately 30–60 kDa between the C terminus of p28 and the N terminus of p50. We speculate that a product of this size may be the first product cleaved from the polyprotein chain of greater than 400 kDa, after the cleavage of p28 but prior to the cleavage of p290.

The specific proteases responsible for the intracellular cleavages of ORF 1a polyprotein precursors have not been identified, but several predictions can be made based on the ORF 1a sequence, the kinetics of synthesis and processing of ORF 1a, and the demonstrated sensitivities of the proteolytic events to inhibitors. The cleavage of p290 from a precursor polyprotein was a delayed event even at late times of infection, suggesting that it may have occurred by an intramolecular or cis proteolytic activity. It is reasonable to postulate that *cis* proteolysis by the predicted 3C-like protease may have been responsible for the cleavage into p290, since it resides between aa3350 and 3652 of ORF 1a, and since greater than 400 kDa of polypeptide was translated before the cleavage occurs in the infected cell. The same reasoning applies to the late cleavage of p290 into p50 and p240, with the exception that this cleavage was quite susceptible to inhibition by leupeptin, suggesting that either an entirely different protease may have been responsible for this delayed cleavage, or that a conformational change may have been necessary before cleavage could occur.

Intracellular translation and processing of ORF 1a products appears to differ from that which occurs during *in vitro* translation in rabbit reticulocyte lysates, where the major N-terminal ORF 1a products were p28, p220, and p250 (Denison and Perlman, 1986). Differences in nonstructural protein synthesis *in vitro* and in infected cells have been described for other RNA viruses, such as poliovirus. However, in the case

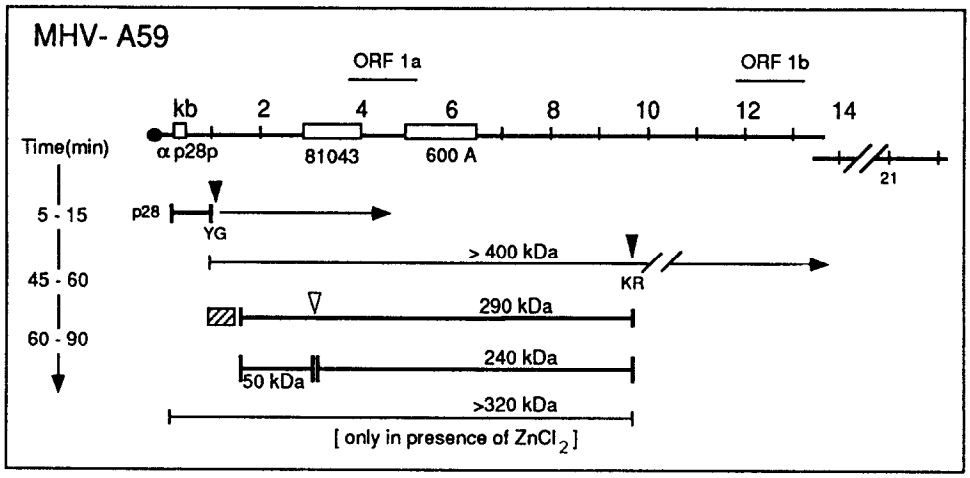

FIG. 6. Suggested model of ORF1a translation and processing in MHV A59-infected cells. The size of ORF 1a, the sequences spanned by the antisera (81043 and 600A), the predicted sizes of the proteins, and the possible cleavage sites are all shown to scale. General alignment of polypeptides is based on antisera specificity and has not been confirmed by protein sequencing, and thus the exact relationships must be considered speculative. The filled triangles and amino acid dipeptides (tyr-gly, lys-arg) indicate previously reported potential ORF 1a cleavage sites which could account for products of the sizes identified. Nonfilled triangles indicate possible cleavage sites for which no dipeptides have been suggested in the literature. None of these cleavage sites has been experimentally confirmed. The times required for the individual cleavages to occur are shown to the left of the diagram. The kinetics of the >320-kDa band, seen by all three antisera only in the presence of protease inhibitor, has not been determined. The hatched rectangle adjacent to p290 indicates a postulated product of 30–60 kDa, which was not identified by the antisera in this study (see Discussion).

of poliovirus the difference in intracellular and *in vitro* synthesis is attributable to internal initiation of translation in the *in vitro* system (Dorner *et al.*, 1984). This does not appear to be the case with MHV, since initiation of ORF 1a translation appears to be primarily N-terminal *in vitro*. The reason for the difference in the pattern of ORF 1a polypeptide synthesis *in vitro* and *in vivo* is not yet clear. In order to more effectively elucidate the differences, we are performing *in vitro* translation using lysates derived from cells permissive for MHV replication.

ACKNOWLEDGMENTS

We thank J. Gombold for helpful discussion, and C. Thorpe and Z. Bielecka for technical assistance. This work was supported by Public Health service Grants R29 AI-26603 (MD), AI-17418 and NS-21954(SW), NS24401 and RCDA NS01369 (SP), and National Multiple Sclerosis Society Grant NMSS RG 2203-A-5 (J.L.L.).

REFERENCES

APPLEYARD, G., and TISDALE, M. (1985). Inhibition of the growth of human coronavirus 229E by leupeptin. *J. Gen. Virol.* **66,** 363–366.

BAKER, S. C., SHIEH, C.-K., SOE, L. H., CHANG, M.-F., VANNIER, D. M., and LAI, M. M. C. (1989). Identification of a domain required for autoproteolytic cleavage of murine coronavirus gene A polyprotein. *J. Virol.* **63,** 3693–3699.

BOURSNELL, M. E. G., BROWN, T. D. K., FOULDS, I. J., GREEN, P. F., TOMLEY, F. M., and BINNS, M. M. (1987). Completion of the sequence of the genome of the coronavirus avian infectious bronchitis virus. *J. Gen. Virol.* **68,** 57–77.

BREEDENBEEK, P. J., PACHUK, C. J., NOTEN, A. F. H., CHARITE, J., LUYTJES, W., WEISS, S. R., and SPAAN, W. J. M. (1990). The primary structure and expression of the second open reading frame of the polymerase gene of the coronavirus MHV-A59: A highly conserved polymerase is expressed by an efficient ribosomal frameshifting mechanism. *Nucleic Acids Res.* **18,** 1825–1832.

BRIERLEY, I., BOURSNELL, M. E. G., BINNS, M. M., BILLIMORIA, B., BLOK, V. C., BROWN, T. D. K., and INGLIS, S. C. (1987). An efficient ribosomal frame-shifting signal in the polymerase encoding region of the coronavirus IBV. *EMBO J.* **6,** 3779–3785.

DE GROOT, R. J., HARDY, W. R., and STRAUSS, J. H. (1990). Cleavage-site preferences of Sindbis virus polyproteins containing the nonstructural proteinase. Evidence for temporal regulation of polyprotein processing in vivo. *EMBO J.* **9,** 2631–2638.

DENISON, M., and PERLMAN, S. (1987). Identification of a putative polymerase gene product in cells infected with murine coronavirus A59. *Virology* **157,** 565–568.

DENISON, M. R., and PERLMAN, S. (1986). Translation and processing of mouse hepatitis virus virion RNA in a cell-free system. *J. Virol.* **60,** 12–18.

DENISON, M. R., ZOLTICK, P. W., LEIBOWITZ, J. L., PACHUK, C. J., and WEISS, S. R. (1991). Identification of polypeptides encoded in open reading frame 1b of the putative polymerase gene of the murine coronavirus mouse hepatitis virus A59. *J. Virol.* **65,** 3076–3082.

DORNER, A. J., SEMLER, B. L., JACKSON, R. J., HANECAK, R., DUPREY, E., and WIMMER, E. (1984). In vitro translation of poliovirus RNA: Utilization of internal initiation sites in reticulocyte lysate. *J. Virol.* **50,** 507–514.

GORBALENYA, A. E., KOONIN, E. V., DONCHENKO, A. P., and BLINOV, V. M. (1989). Coronavirus genome: prediction of putative functional domains in the nonstructural polyprotein by comparative amino acid sequence analysis. *Nucleic Acids Res.* **17,** 4847–4861.

GORDON, P. B., and SEGLEN, P. O. (1989). *in* "Proteolytic Enzymes: A

Practical Approach." (R. J. Benyon and J. S. Bond, Eds.), pp. 201–210. IRL Press, Oxford.

KRAUSSLICH, H.-G., and WIMMER, E. (1988). Viral proteinases. *Annu. Rev. Biochem.* **57,** 701–754.

LAEMMLI, U. K. (1970). Cleavage of structural proteins during the assembly of the head of bacteriophage T4. *Nature* **227,** 680–685.

LAMBLIN, P. (1978). Reliability of molecular weight determination of proteins by polyacrylamide gradient gel electrophoresis in the presence of sodium dodecyl sulfate. *Anal. Biochem.* **85,** 114–125.

LAMBLIN, P., and FINE, J. M. (1979). Molecular weight estimation of proteins by electrophoresis in linear polyacrylamide gradient gels in the absence of denaturing agents. *Anal. Biochem.* **98,** 160–168.

LAMBLIN, P., ROCHU, D., and FINE, J. M. (1976). A new method for determination of molecular weights of proteins by electrophoresis across a sodium dodecyl sulfate (SDS)–polyacrylamide gradient gel. *Anal. Biochem.* **74,** 567–575.

LEE, H.-J., SHIEH, C.-K., GORBALENYA, A. E., KOONIN, E. V., LAMONICA, N., TULER, J., BAGDZHADHZYAN, A., and LAI, M. M. C. (1991). The complete sequence (22 kilobases) of murine coronavirus gene 1 encoding the putative proteases and RNA polymerase. *Virology* **180,** 567–582.

LEIBOWITZ, J. L., WEISS, S. R., PAAVOLA, E., and BOND, C. W. (1982). Cell-free translation of murine coronavirus RNA. *J. Virol.* **43,** 903–913.

PACHUK, C. J., BREEDENBEEK, P. J., ZOLTICK, P. W., SPAAN, W. J. M., and WEISS, S. R. (1989). Molecular cloning of the gene encoding the putative polymerase of mouse hepatitis coronavirus, strain A59. *Virology* **171,** 141–148.

PALMENBURG, A. C. (1990). Proteolytic processing of picornaviral polyprotein. *Annu. Rev. Microbiol.* **44,** 603–623.

PERLMAN, S., REESE, D., BOLGER, E., CHANG, L. J., and STOLTZFUS, C. M. (1987). MHV nucleocapsid synthesis in the presence of cycloheximide and accumulation of negative strand MHV RNA. *Virus Res.* **6,** 261–272.

SABORIO, J. L., PONG, S.-S., and KOCH, G. (1974). Selective and reversible inhibition of initiation of protein synthesis in mammalian cells. *J. Mol. Biol.* **85,** 195–211.

SAWICKI, D. L., and SAWICKI, S. G. (1986). Coronavirus minus-strand RNA synthesis and effect of cycloheximide on coronavirus RNA synthesis. *J. Virol.* **57,** 328–334.

SOE, L. H., SHIEH, C.-K., BAKER, S. C., CHANG, M.-F., and LAI, M. M. C. (1987). Sequence and translation of the murine coronavirus 5′-end genomic RNA reveals the N-terminal structure of the putative RNA polymerase. *J. Virol.* **61,** 3968–3976.

ZOLTICK, P. W., LEIBOWITZ, J. L., DE VRIES, J. R., WEINSTOCK, G. M., and WEISS, S. R. (1989). A general method for the induction and screening of antisera for cDNA-encoded polypeptides: antibodies specific for a coronavirus putative polymerase-encoding gene. *Gene* **85,** 413–420.